Status report about the Drift Chamber project for the future collider

Nicola De Filippis
Politecnico and INFN Bari

on behalf of the DCH community

2023 International Workshop on the High Energy Circular Electron Positron Collider

Nanjing 23-27, 2023

European network for developing new horizons for RIs

This project has received funding from the European Union's Horizon 2020 research and innovation programme under grant agreement No. 871072

This project has received funding from the European Union's Horizon 2020 Research and Innovation programme under GA no 101004761.

The IDEA detector at e^+e^- colliders

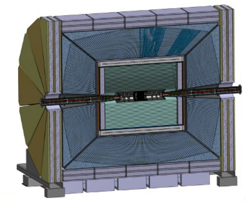

Innovative Detector for E+e- Accelerator

IDEA consists of:

- a silicon pixel vertex detector
- a large-volume extremely-light **drift chamber**
- surrounded by a layer of silicon micro-strip detectors
- a thin low-mass superconducting solenoid coil
- a preshower detector based on **□-WELL technology**
- a dual read-out calorimeter
- muon chambers inside the magnet return yoke, based on **□-WELL technology**

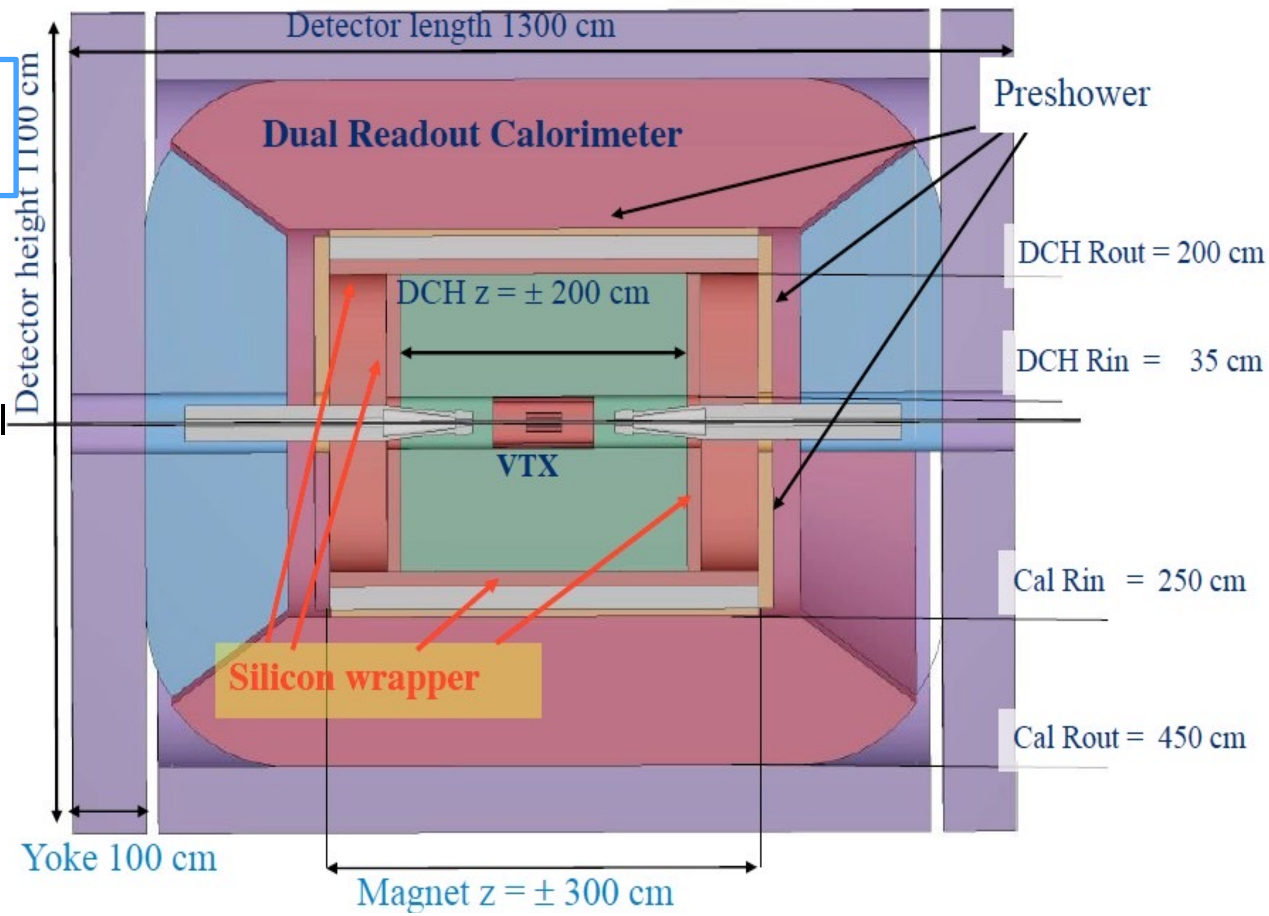

Low field detector solenoid to maximize luminosity (to contain the vertical emittance at Z pole).

→ optimized at 2 T

→ large tracking radius needed to recover momentum resolution

The Drift Chamber of IDEA

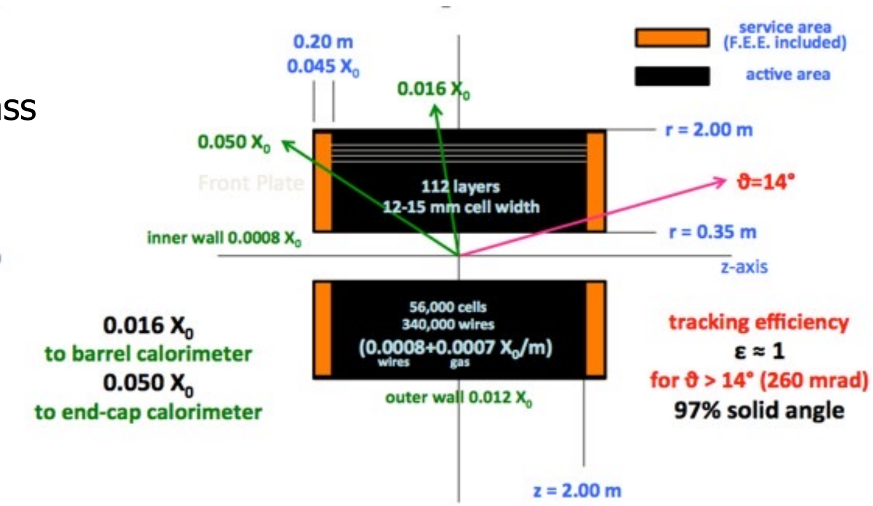

The DCH is:

- a unique-volume, high granularity, fully stereo, low-mass cylindrical
- gas: He 90% - iC_4H_{10} 10%
- inner radius R_{in} = 0.35m, outer radius R_{out} = 2m
- length L = 4m
- drift length ~1 cm
- drift time ~150ns
- σ_{xy} < 100 μm, σ_z < 1 mm
- 12÷14.5 mm wide square cells, 5 : 1 field to sense wires ratio
- 112 co-axial layers, at alternating-sign stereo angles, arranged in 24 identical azimuthal sectors, with frontend electronics
- 343968 wires in total:

  sense vires: 20 μm diameter W(Au) =>56448 wires

  field wires: 40 μm diameter Al(Ag) =>229056 wires

  f. and g. wires: 50 μm diameter Al(Ag) => 58464 wires

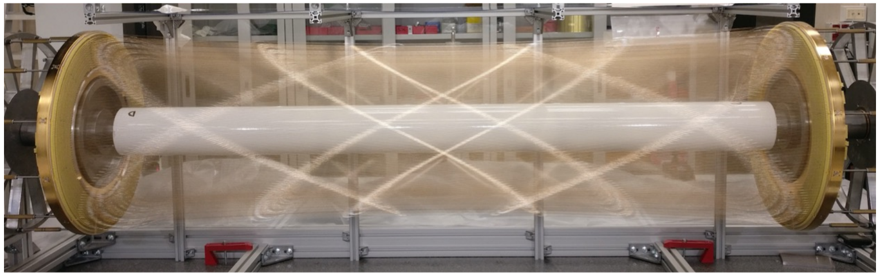

- the wire net created by the combination of + and – orientation generates a more uniform equipotential surface → better E-field isotropy and smaller ExB asymmetries)

- thin wires → increase the chamber granularity → reducing both multiple scattering and the overall tension on the endplates

Challenges for large-volume drift chambers

- **Electrostatic stability** condition: $\frac{\lambda^2}{4\pi\varepsilon}\frac{L^2}{w^2} < wire\ tension < YTS \cdot \pi r_w^2$

λ = linear charge density (gas gain)
L = wire length, r_w wire radius, w = drift cell width
YTS = wire material yield strength

The proposed drift chambers for FCC-ee and CEPC have lengths **L = 4 m** and plan to exploit the cluster counting technique, which requires gas gains **~5×10^5**.
This poses serious constraints on the drift cell width (**w**) and on the wire material (**YTS**).

⇒ new wire material studies

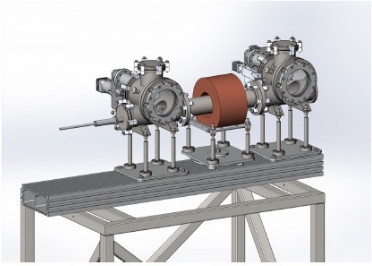

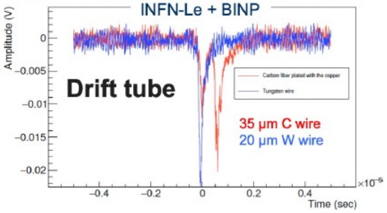

- **Non-flammable gas / recirculating gas systems**
Safety requirements (**ATEX**) demands stringent limitations on flammable gases;
Continuous increase of **noble gases cost**

⇒ gas studies

- **Data throughput**
Large number of channels, high signal sampling rate, long drift times (slow drift velocity), required for cluster counting, and high physics trigger rate (Z_0-pole at FCC-ee) imply data transfer rates in excess of **~1 TB/s**

⇒ on-line real time data reduction algorithms

- **New wiring systems for high granularities / / new end-plates / new materials**

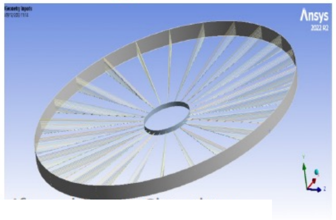

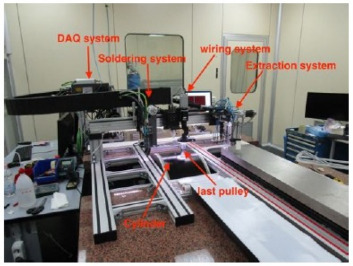

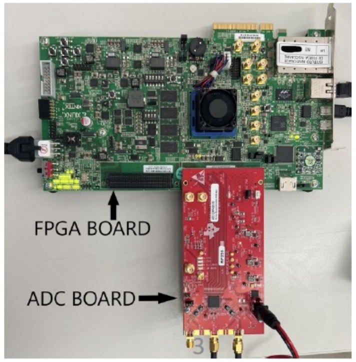

Mechanical design of the DCH

Mechanical structure

New concept of construction allows to reduce material to $\approx 10^{-3}\ X_0$ for the barrel and to a few x $10^{-2}\ X_0$ for the end-plates.

- separation of functions

Gas containment
Gas vessel can freely deform without affecting the internal wire position and mechanical tension.

Wire cage
Wire support structure not subject to differential pressure can be light and feed-through-less

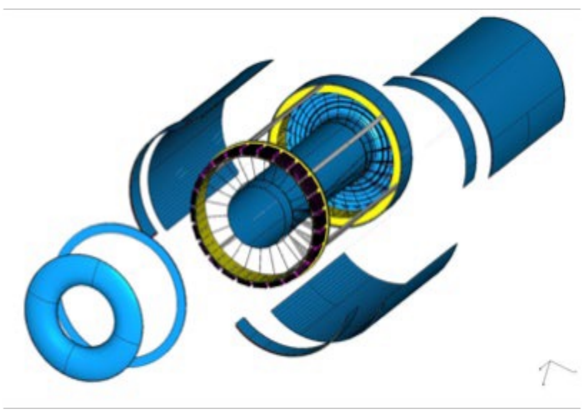

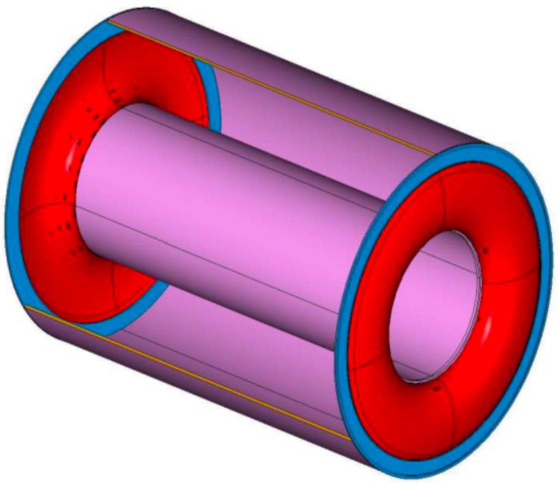

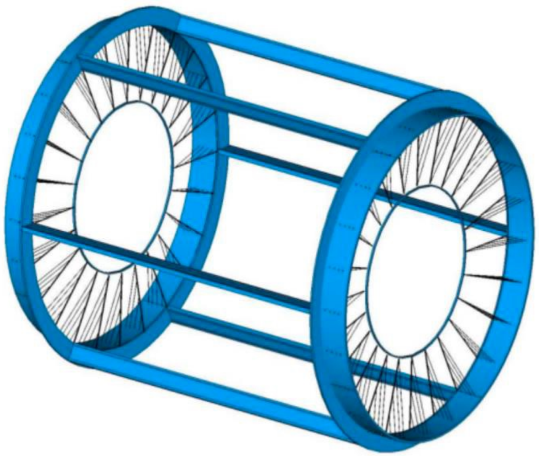

Mechanical structure: wire cage

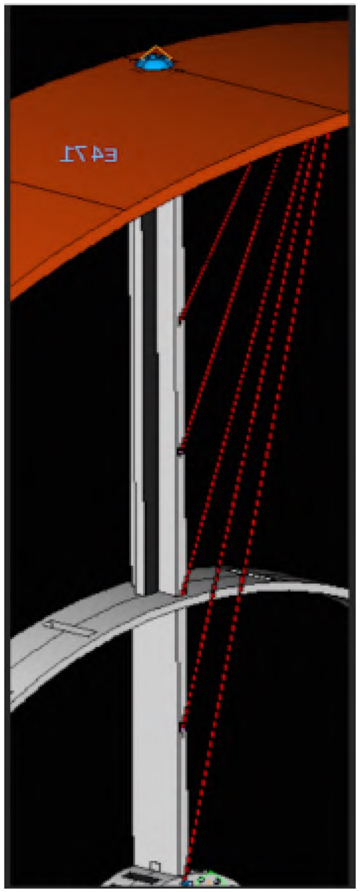

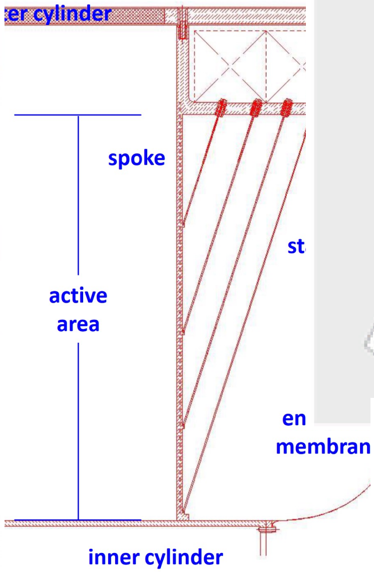

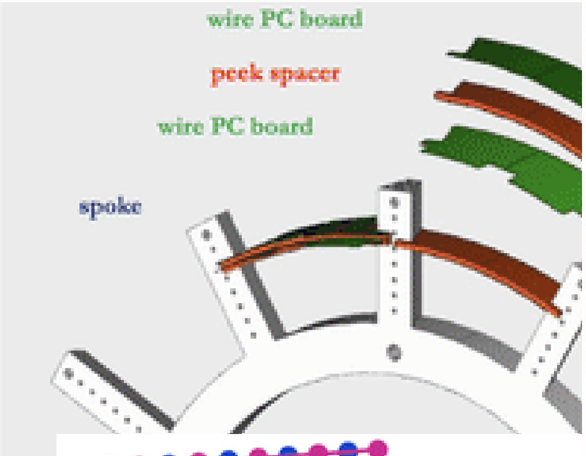

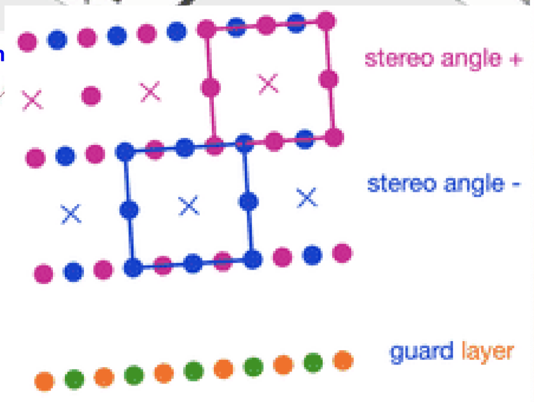

Mechanical structure: layout

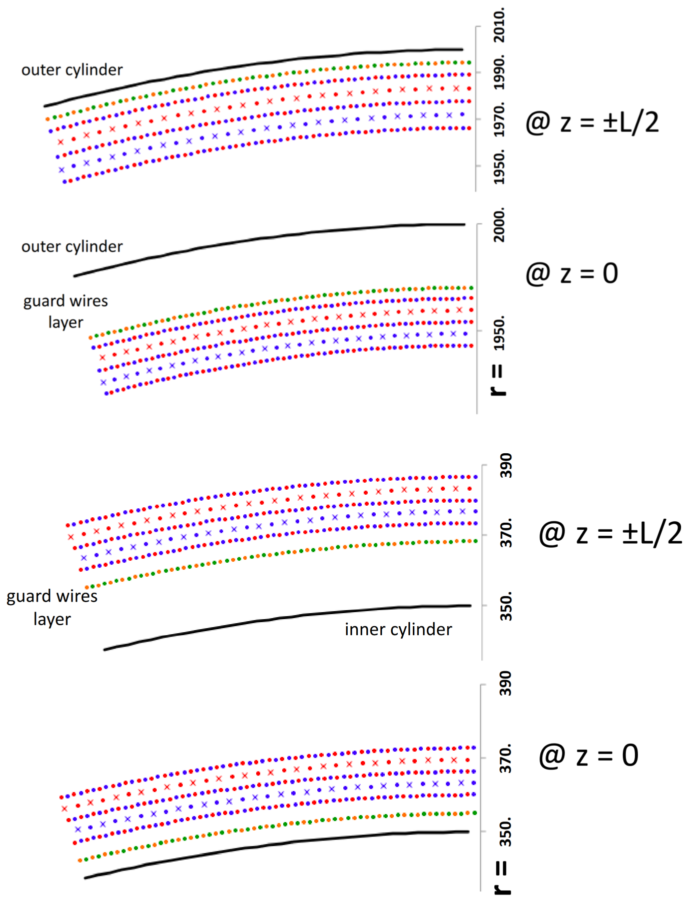

Radii (at z = 0)		
Inner Cylinder	350	mm
Guard wires layer	354	mm
First active layer	356	mm
Last (112[th]) active layer	1915	mm
Guard wires layer	1927	mm
Outer Cylinder	2000	mm

Radii (at end plate)		
Inner Cylinder	350	mm
Guard wires layer	366	mm
First active layer	369	mm
Last (112[th]) active layer	1982	mm
Guard wires layer	1995	mm
Outer Cylinder	2000	mm

Active length	2000	mm
Number of super-layers (8 layers) Number of sectors	(14x8) = 112 24	
Number of cells per layer / per sector	192÷816 / 16	
Cell size (at z=0)	11.8 ÷ 14.9	mm
2α angle	30°	
Stereo angle	43 ÷ 223	mrad
Stereo drop	12.5 ÷ 68.0	mm

sense wires	56 448
field wires	284 256
guard wires	2 016
Total wires	342 720

Challenges:

- the accuracy of the position has to be in the range of 100-200 μm
- the position of the anodic wire in space must be known with an accuracy better than 50μm at most
- the anodic and cathodic wires should be parallel in space to preserve the uniformity of the electric field
- a 20μm tungsten wire, 2m long, will bow about 100 μm at its middle point, if tensioned with a load of approximately 30gr → 30gr tension for each wire → 10 tons of total load on the endcap → simulation studies with FEM

Mechanical structure: the FEM simulation

Parametric Design exploration: varying input parameters in some possible ranges in order to see how the system responds - Response Surface Methodology (RSM) is used.

The input parametric variables are:

1. Height and thickness of the outer cylinder;
2. Dimensions (breadth and depth) of the spokes;
3. Dimensions (radius) of the cables;
4. Thickness of the inner cylinder.

Change the material: from carbon fiber to Epoxy Carbon Unidirectional Prepeg

- select the optimal dimensions of the drift chamber
- **total deformation of the model from 135,03 mm to 21,64 mm → still too high!**

Parameters:	
Height:	200 mm
Innerthickness:	10 mm
Outerthickness:	14.4 mm
Rectangle_B:	9.6 mm
Rectangle_H:	16.6 mm
Circle_R:	1.5 mm

Responses:	
Maximum_Deformation:	22.995 mm (Linear Analysis)
Maximum_Deformation:	21.643 mm (Non-Linear Analysis)
Total_Mass:	2.6269 kg per sector
Total_Deformation_Load_Multiplier:	2.2068

Mechanical structure: prestressing

Goal: minimizing the deformation of the spokes using prestressing force in the cables

Finding the correct prestressing force in 14 cables → solving 15 dimensional optimization problem

Total deformation (mm) of the drift chamber with the edge of the outer cylinders fixed			
No prestress		Prestress in the cables	
Spokes	Outer cylinder	Spokes	Outer cylinder
14.099	0.63	0.62	0.67

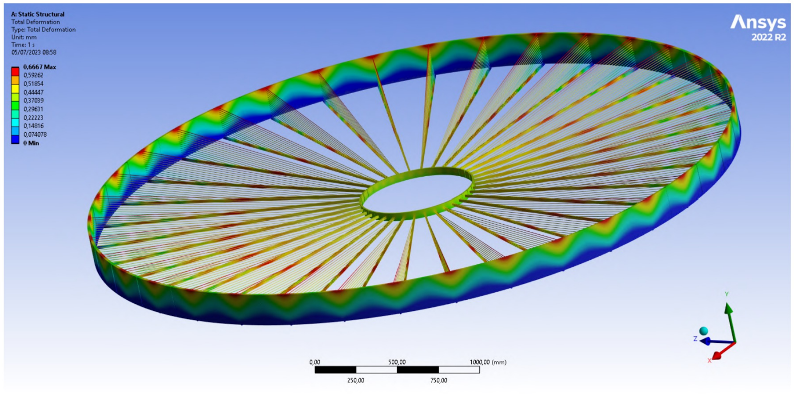

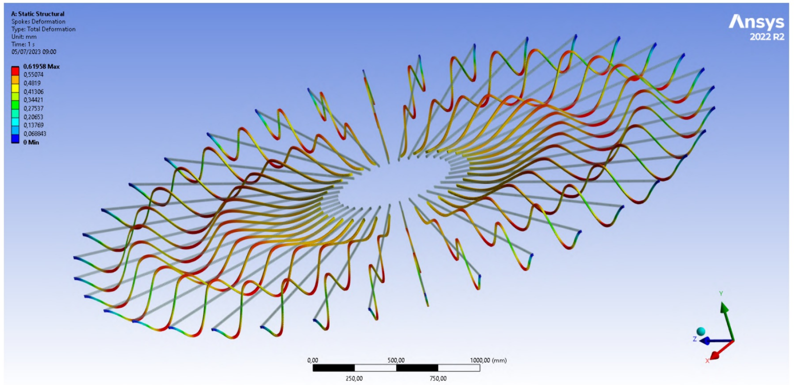

N.B.

- Prestressing not yet optimized
- 24 → 36 spokes considered for this study

The structure exhibited a deformation of 600 µm but our goal was to limit the deformation of the spokes to 200 µm while ensuring the structural integrity.

Mechanical structure: a complete model

A realistic complete model almost ready:

- mechanically accurate
- precise definition of the connections of the cables on the structure
- connections of the wires on the PCB
- location of the necessary spacers
- connection between wire cage and gas containment structure

→

the final project will be ready by the end of 2023

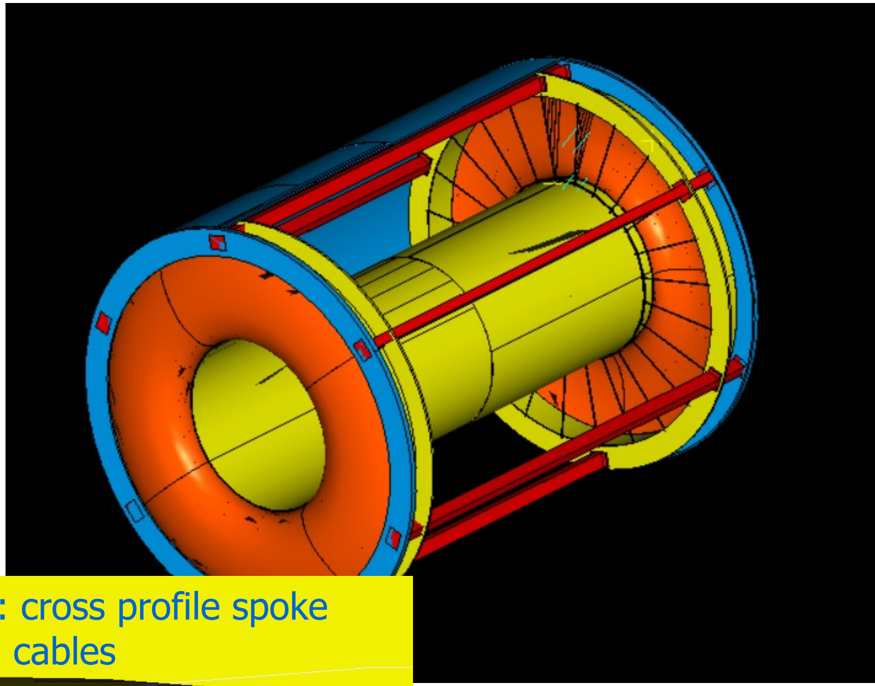

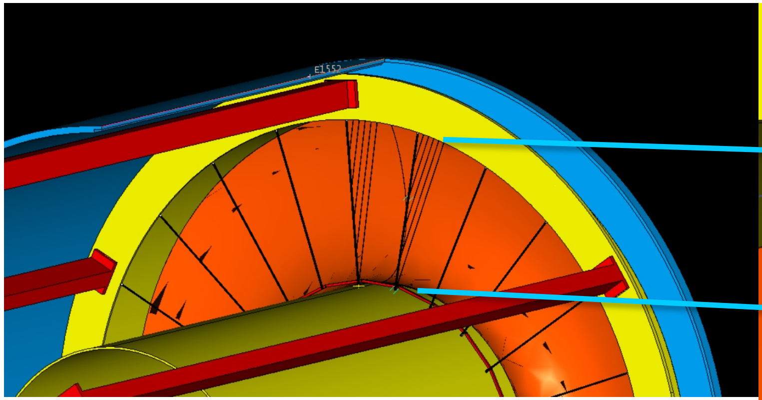

Upper junction: cross profile spoke and supporting cables

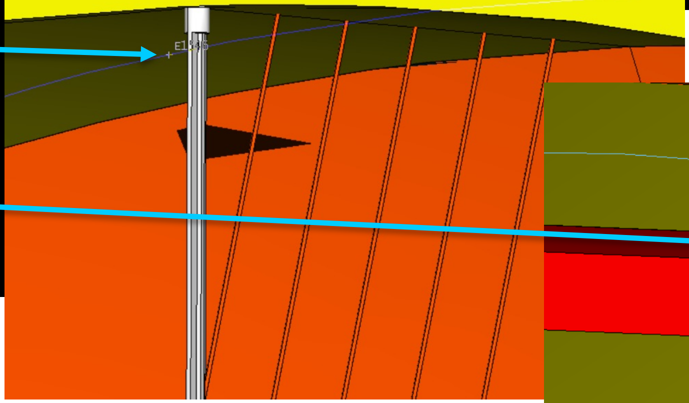

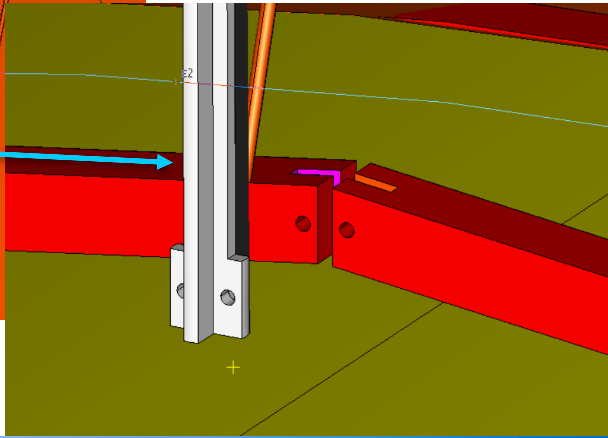

Plan to start the construction of a DCH prototype full lenght, one sector, next year.

Lower junction: joint design

Testbeam data analysis

The Drift Chamber: Cluster Counting/Timing and PID

Principle: In He based gas mixtures the signals from each ionization act can be spread in time to few ns. With the help of a fast read-out electronics they can be identified efficiently.

- By counting the number of ionization acts per unit length (dN/dx), it is possible to identify the particles (P.Id.) with a better resolution w.r.t the dE/dx method.

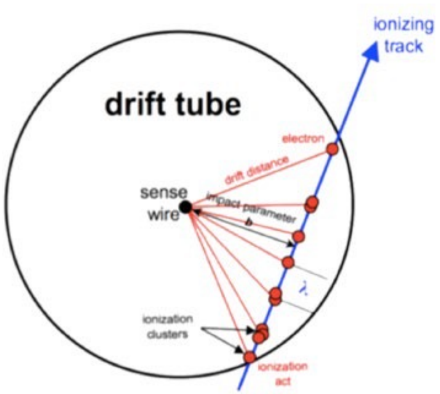

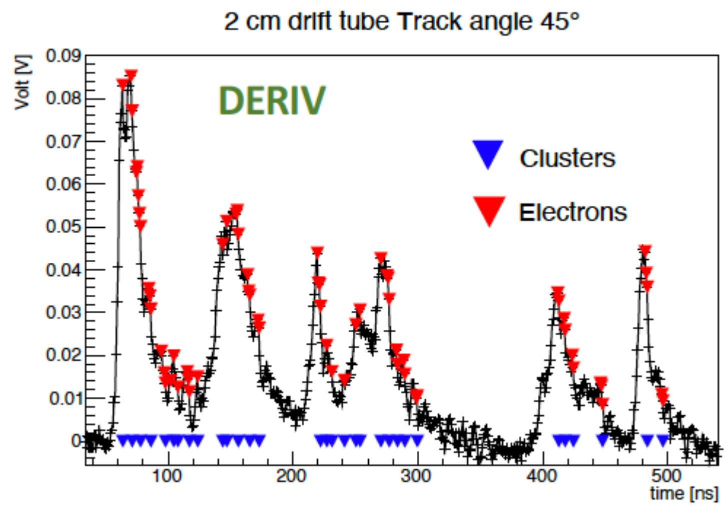

- collect signal and identify peaks
- record the time of arrival of electrons generated in every ionisation cluster
- reconstruct the trajectory at the most likely position

- Landau distribution of dE/dx originated by the mixing of primary and secondary ionizations, has large fluctuations and limits separation power of PID → primary ionization is a Poisson process, has small fluctuations

- The cluster counting is based on replacing the measurement of an ANALOG information (the [truncated] mean dE/dX) with a DIGITAL one, the number of ionisation clusters per unit length:

dE/dx: truncated mean cut (70-80%), with a 2m track at 1 atm give $\sigma \approx 4.3\%$

dN_{cl}/dx: for $He/iC_4H_{10}=90/10$ and a 2m track gives $\sigma_{dNcl/dx}/(dN_{cl}/dx) < 2.0\%$

The Drift Chamber: Cluster Counting/Timing and PID

- Analitic calculations: Expected excellent K/π separation over the entire range except 0.85<p<1.05 GeV (blue lines)

- Simulation with Garfield++ and with the Garfield model ported in GEANT4:
  - the particle separation, both with dE/dx and with dN_{cl}/dx, in GEANT4 found considerably worse than in Garfield
  - the dN_{cl}/dx Fermi plateau with respect to dE/dx is reached at lower values of βγ with a steeper slope
  - finding answers by using real data from beam tests

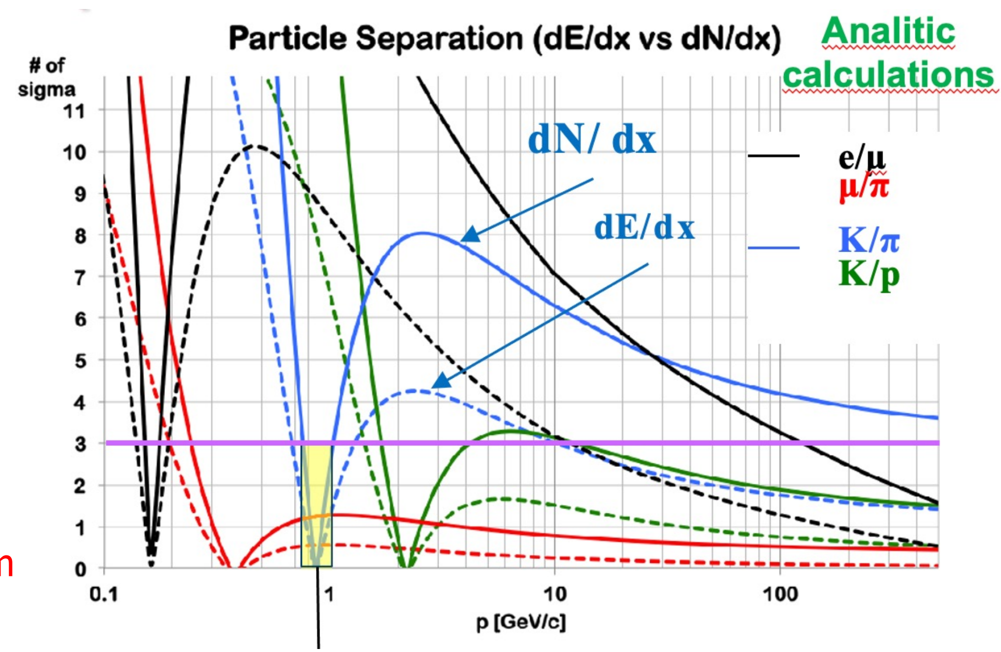

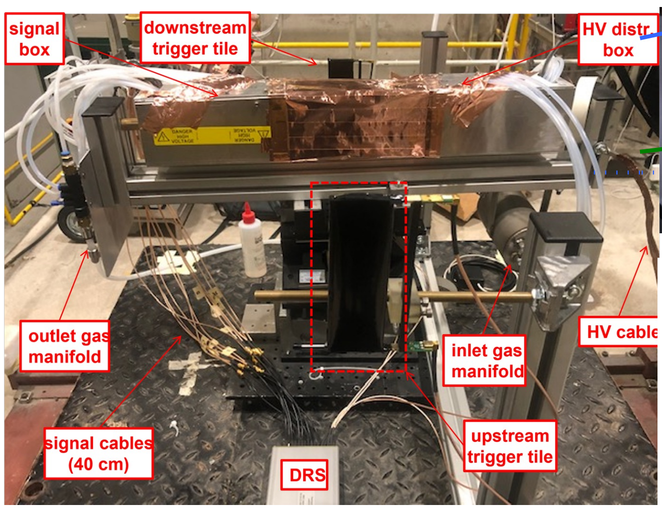

90%He-10%iC_4H_{10}
nominal HV+20, 45°,
Gas gain ~ 2 · 10^5,
165 GeV/c

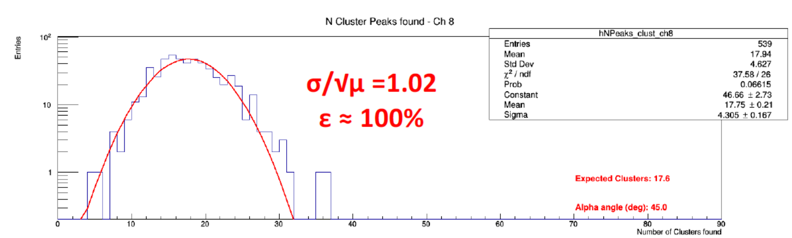

- Poissonian behaviour of the number of clusrers

- Meaurements vs predictions about the number of clusters are in very good agreement

- Same results in independent drift tubes

Beam tests in 2021,2022 and 2023

Beam tests to experimentally asses and optimize the **performance of the cluster counting/timing** techniques in close collaboration with the IHEP Beijing group:

- Two **muon beam tests** performed at **CERN-H8 (βγ > 400)** in Nov. 2021 and July 2022.
- A **muon beam test** (from 4 to 12 GeV momentum) in 2023 performed at **CERN**.
- Ultimate test at **FNAL-MT6** in 2024 with π and **K (βγ = 10−140)** to fully exploit the relativitic rise.

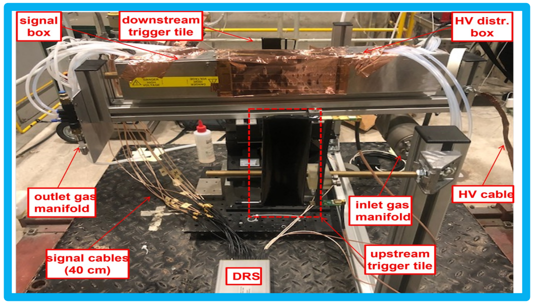

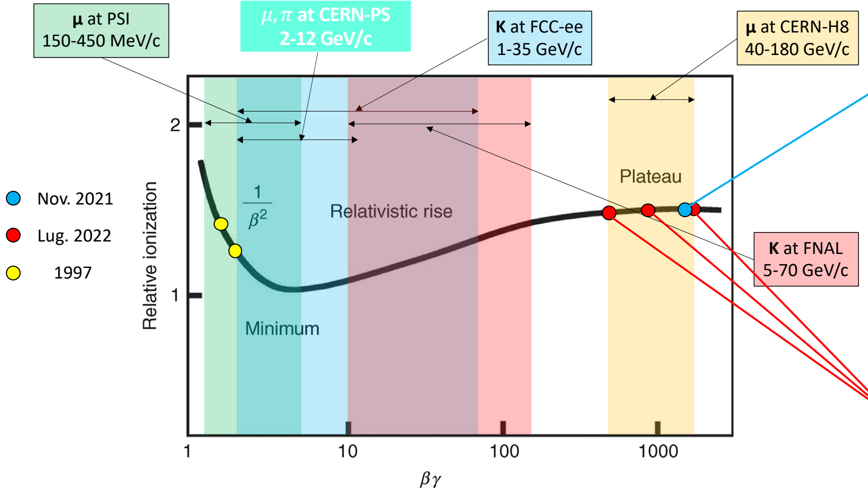

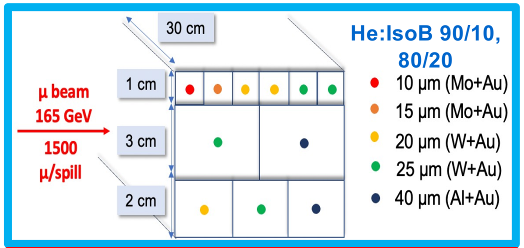

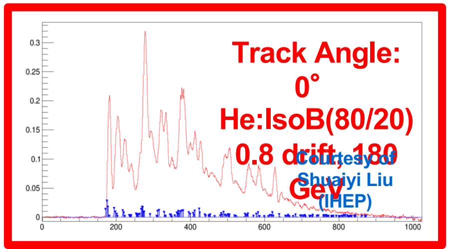

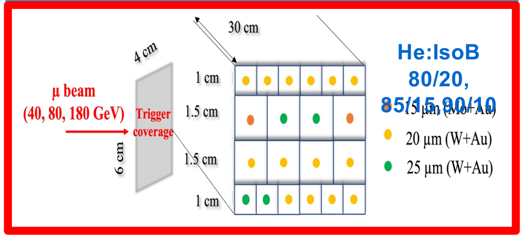

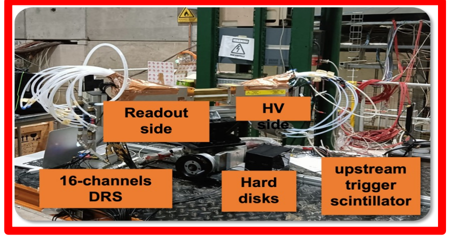

2021/2022 testbeam: find electron peaks algorithms

Find good electron peak candidates at position bin *n* and amplitude A_n:

FIRST AND SECOND DERIVATIVE (DERIV) ALGORITHM

- Compute the first and second derivative from the amplitude average over two consecutive bins (1.6 ns for 1.2 GSa/s) and require that, at the peak candidate position, they are smaller than a r.m.s. signal-related small quantity and they increase (decrease) before (after) the peak candidate position of a r.m.s. signal-related small quantity.

- Require that the amplitude at the peak candidate position is larger than a r.m.s. signal-related small quantity and the amplitude difference among the peak candidate and the previous (next) signal amplitude is larger (smaller) than a r.m.s. signal-related small quantity.

NOTE:

- R.m.s. is a measurement of the noise level in the analog signal

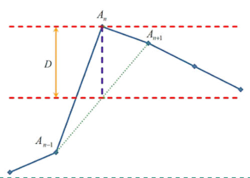

0°, nominal HV+20, 90%He-10%iC_4H_{10}
Tube with 1-cm cell size and 20 µm diameter

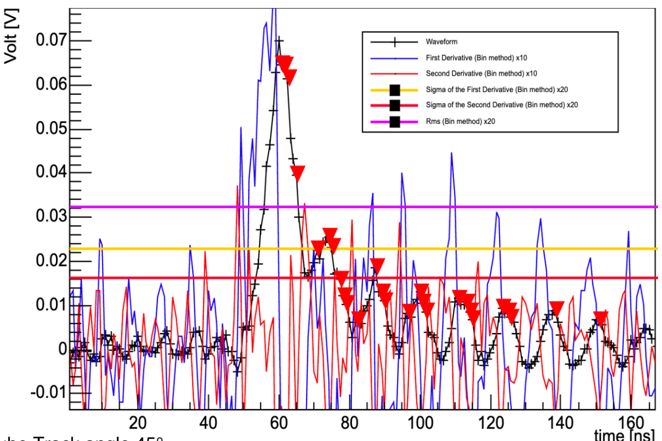

2 cm drift tube Track angle 45°

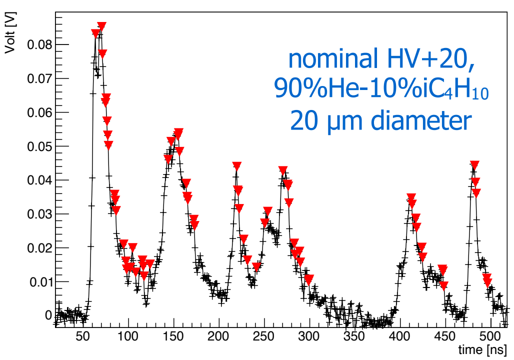

1 cm drift tube Track angle 45°

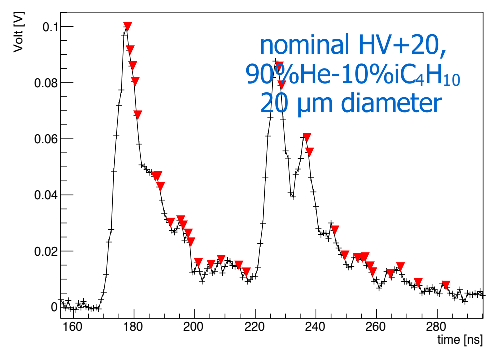

2021/2022 testbeam: find electron peaks algorithms

Find good electron peak candidates at position bin n and amplitude A_n:

RUNNING TEMPLATE ALGORITHM (RTA)

- Define an electron pulse template based on experimental law with a raising and falling exponential over a fixed number of bins (K_{tot}) and digitized ($A(k)$) according to the data sampling rate.
- Run over K_{tot} bins by comparing it to the subtracted and normalized data (build a sort of χ^2 and define a cut on it).
- Subtract the found peak to the signal spectrum and iterate the search and stop when no new peak is found.

k	A(k)
0	0.0
1	0.269
2	1.0
3	0.744
4	0.545
5	0.390
6	0.269
7	0.175
8	0.102
9	0.044
10	0.0

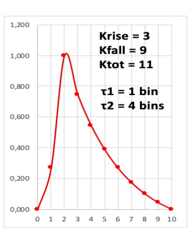

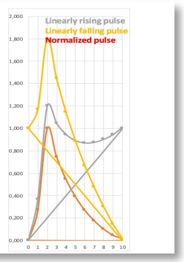

30°, nominal HV+20, 90%He-10%iC_4H_{10}
Tube with 1 cm cell size and 20 μm diameter

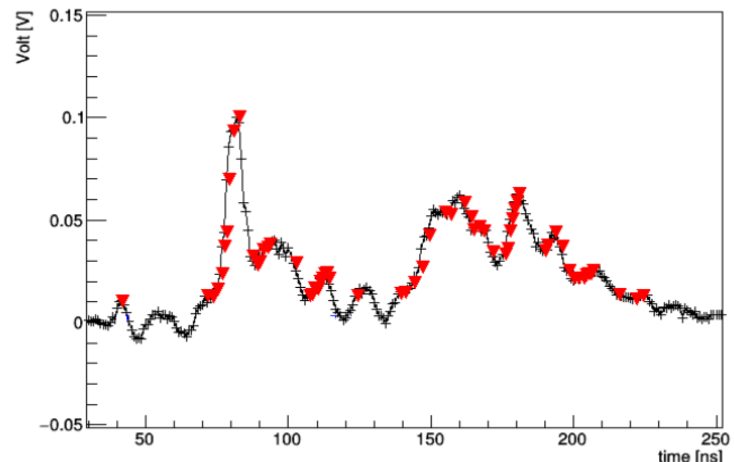

2 cm drift tube Track angle 45°

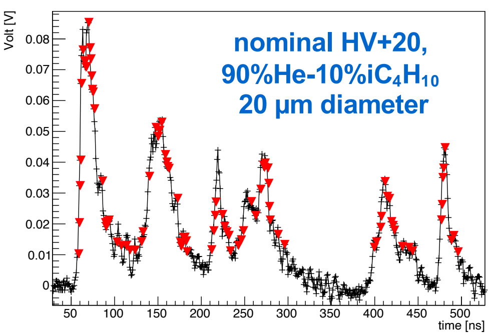

1 cm drift tube Track angle 45°

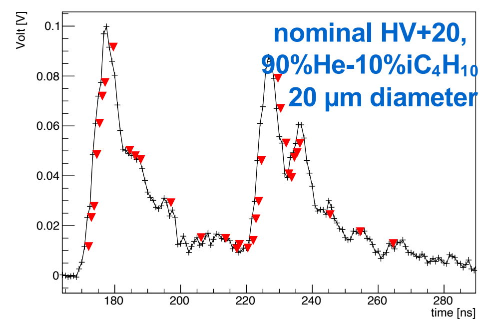

NEW results obtained by using the RTA algorithm

2021/2022 testbeam: number of clusters

Sense Wire Diameter 15 μm; Cell Size 1.0 cm; Track Angle 45; Sampling rate 2 GSa/s; Gas Mixture He:IsoB 80/20

Poissonian distribution for the number of clusters

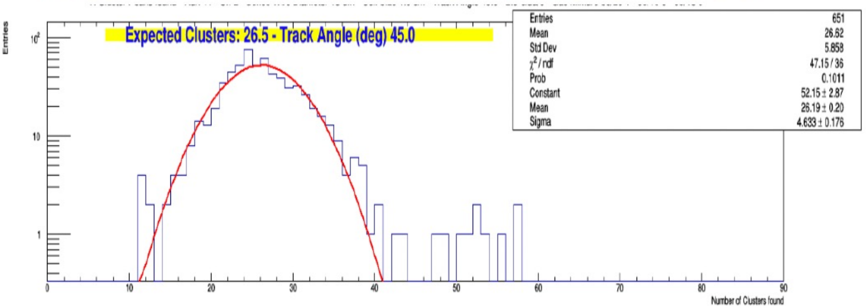

Electrons per cluster distribution

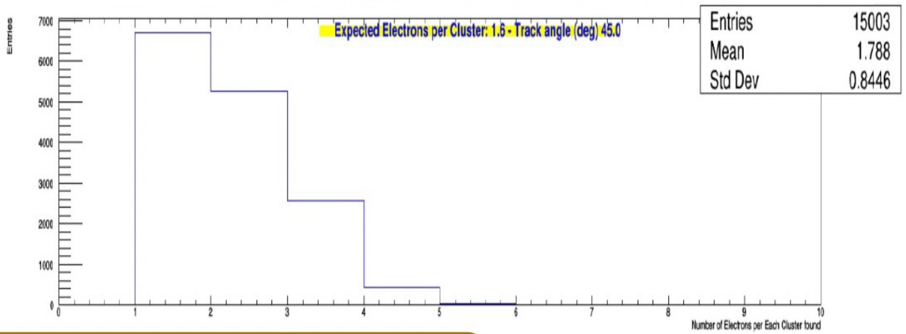

Expected number of cluster = δ cluster/cm (M.I.P.) * drift tube size [cm] * 1.3 (relativistic rise)* 1/cos(α)

α = angle of the muon track w.r.t. normal direction to the sense wire.
δ cluster/cm (mip) changes from 12, 15, 18 respectively for He:IsoB 90/10, 85/15 and 80/20 gas mixtures.
drift tube size are 0.8, 1.2, and 1.8 respectively for 1 cm, 1.5 cm, and 2 cm cell size tubes.

Poissonian distribution of the number of clusters and cluster size in acceptance with the expectation

2021/2022 testbeam: DERIV vs RTA algorithms

1 cm drift tubes

Run: 41; Track angle:45^0; Gas mixture:80% He 20% iC_4H_{10} ; HV = Nominal Sampling rate= 2 Gsa/s

DERIV Algorithm

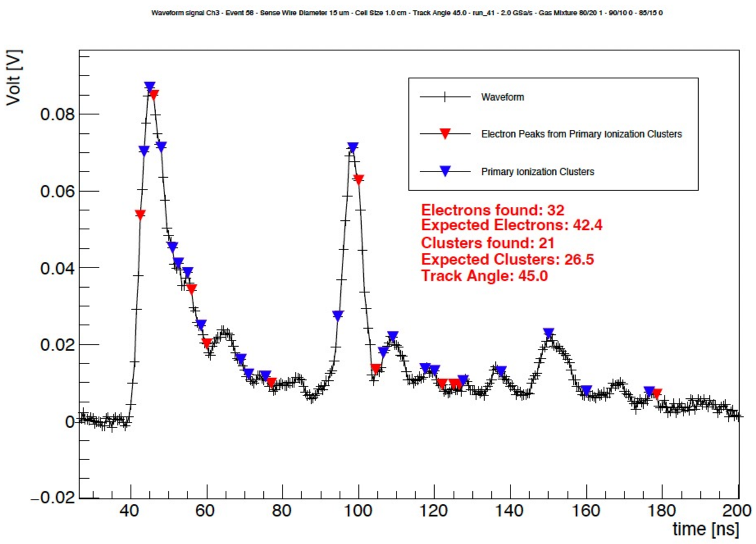

RTA Algorithm

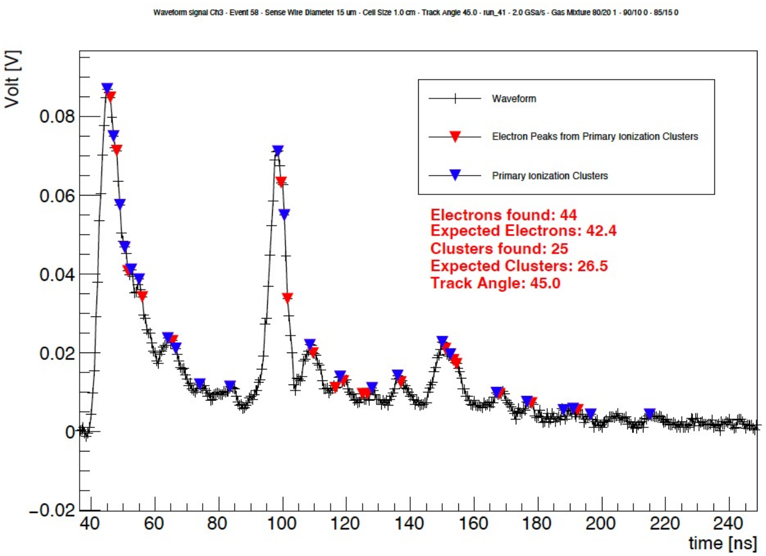

More details were given at ECFA workshop in Paestum

Beam test results: recombination and attachment

Space charge + attachment + recombination effects affect the experimental CC efficiency!

- The **loss of efficiency at small angles** is due to the partial shielding of the electric field due to the space charge.
- The **loss of efficiency at large angles** is partially due to the fact that increasing the number of clusters in the same drift time, increases the probability of pileup, then decreasing the counting efficiency.
- The **lower counting efficiency in 2cm** tubes compared to 1cm ones is only partially explained by the effects of recombination and attachment; other possible effects under investigation

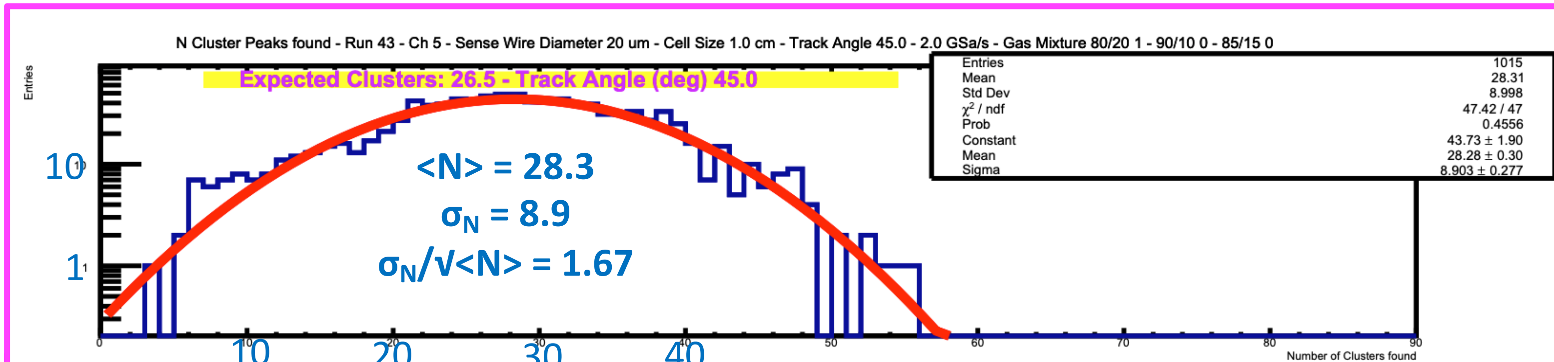

Number of Clusters found by DERIV+CLUSTER algorithms

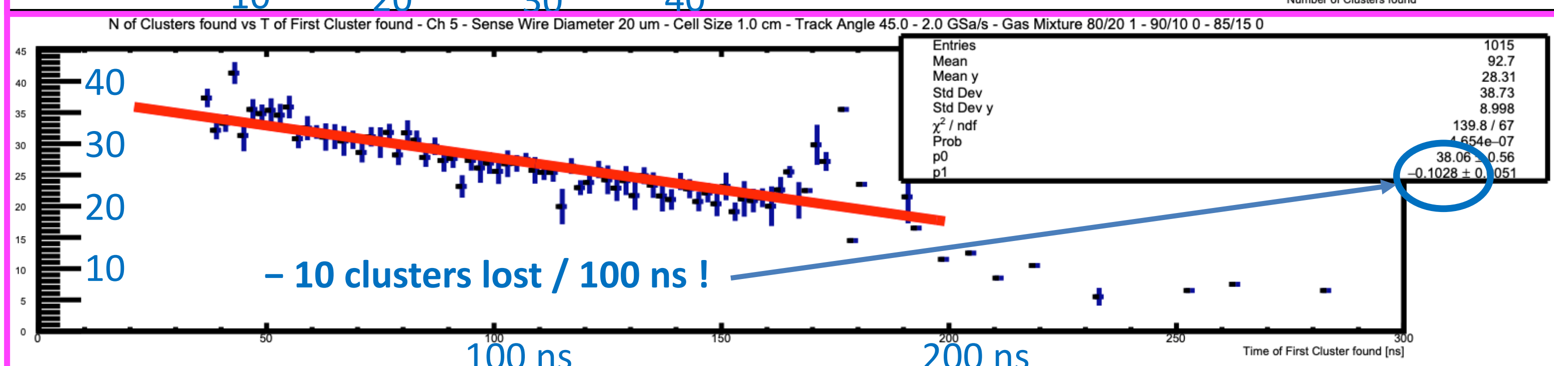

Average Number of Clusters found(@drift time) vs drift time

Combined action of recombination, electron attachment and E-field suppression due to space charge

Beam test results: applying corrections

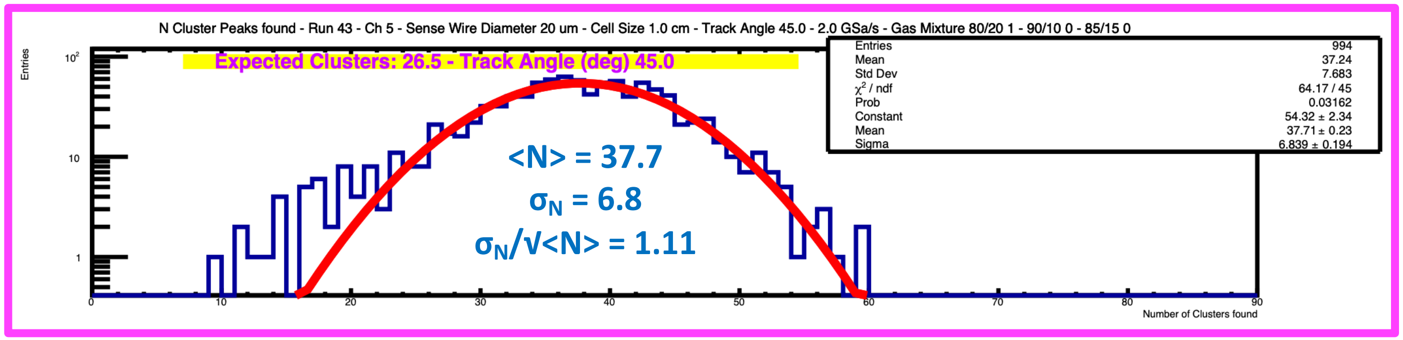

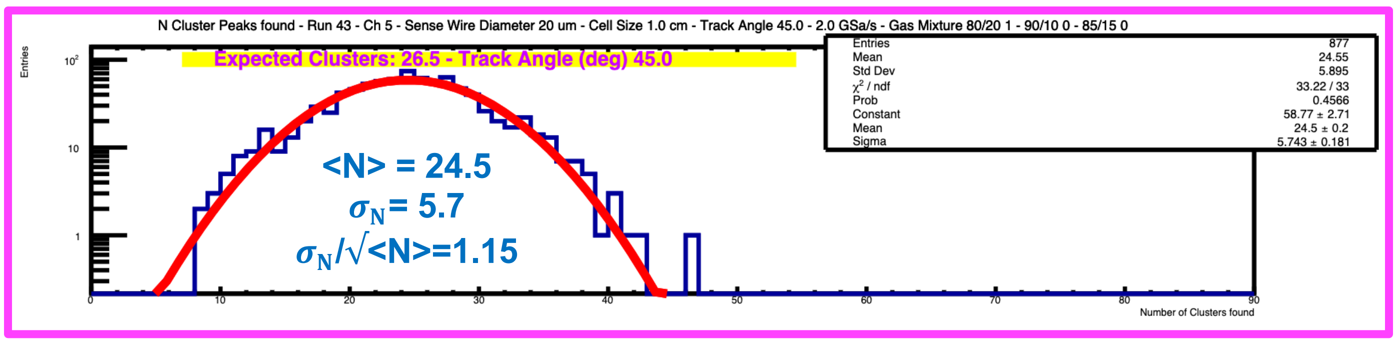

Cuts on the derivative algorithm, which were optimized without including the recombination and attachment effects, need to be reformulated.
Also, these corrections, strongly depend on the drift length and, therefore, on the drift tube size and must be calculated for each different drift tube configuration.

First attempt of re-tuning cuts on the DERIV algorithm for a 1 cm cell size drift tube

Cluster counting with machine learning

The algorithm is under development at IHEP, for more information see [this talk] by Guang ZHAO.

Peak finding with LSTM

Why LSTM? Waveforms are time series

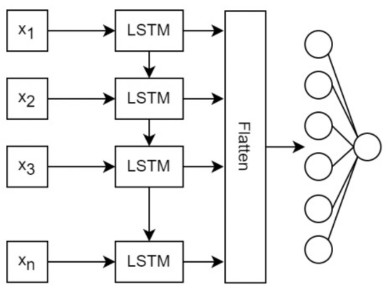

- Architecture: LSTM (RNN-based)
- Method: Binary classification of signals and noises on slide windows of peak candidates

LSTM: Long Short-Term Memory

Clusterization with DGCNN

Why DGCNN? Locality of the electrons in the same primary cluster, perform massage passing through neighbour nodes in GNN

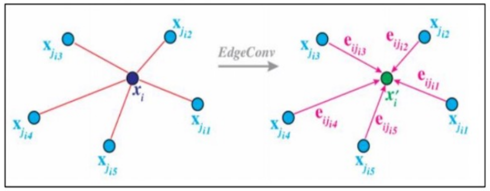

arXiv: 1801.07829

- Architecture: DGCNN (GNN-based)
- Method: Binary classification of primary and secondary electrons

DGCNN: Dynamic Graph Convolutional neural networks

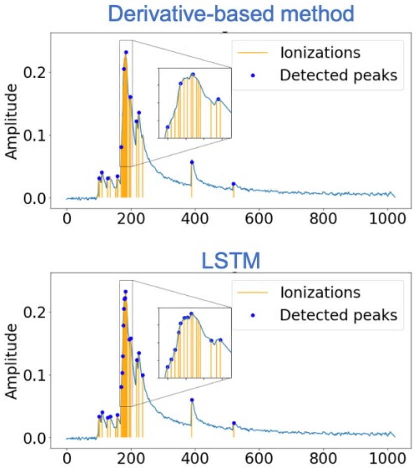

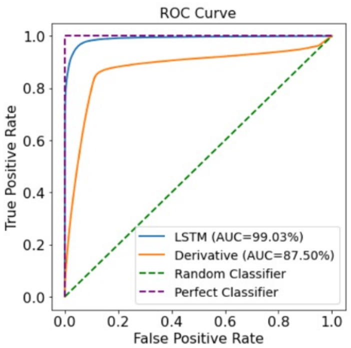

LSTM model is better classifier compared to derivative-based model

Data reduction and preprocessing

Data reduction and pre-processing of DCH signals

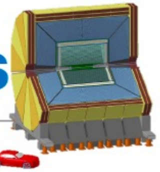

High speed digitization (2 GSa/s) for CC ⟹ Transfer rate of TB/s

- **Data reduction strategy:** transfer, for each hit drift cell, only the minimal information relevant to apply the **Cluster Counting/Timing (CCT) techniques**, i.e. the **amplitude** and the **arrival time of each peak** associated with **each individual ionisation electron** ⟹ **CCT algorithms!**

  ► Use of a **FPGA** for the **real-time data analysis** of drift chamber signals **digitized by an ADC.** Acquire the signals converted ⟹ process with cluster counting algorithms (aimed also at **reducing the data throughput**) ⟹ send the processed information to a back-end computer via an Ethernet interface.

- A fast read-out CCT algorithm has been developed as **VHDL/Verilog** code implemented on a **Virtex 6 FPGA (maximum input/output clock switching frequency** of **710 MHz)**. The hardware setup includes also a **12-bit monolithic pipeline sampling ADC** at conversion rates up to **2.0 GSPS.**

Goal

To implement on FPGA more sophisticated peak finding algorithms for the **parallel pre-processing** of **many ADC channels**:

- **reduce costs** and **system complexity**
- **gain on flexibility in determining proximity correlations** among hit cells for track segment finding and triggering purposes.

Implemtend using a **single channel ADC**

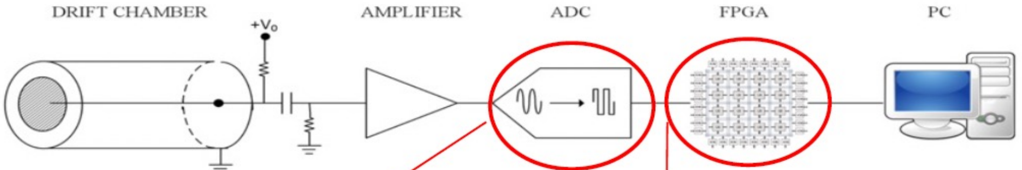

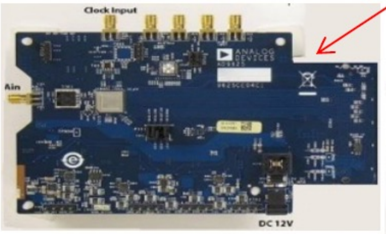

Cluster counting on a FPGA

- We implemented successfully the CCT technique on **a single-channel ADC**
- To implement the multi-channel DCH signals reading, different digitizers are under test:
  1) ADC TEXAS INSTRUMENT **ADC32RF45**
  2) CAEN **digitizer**
  3) NALU SCIENTIFIC **ASoCv3**

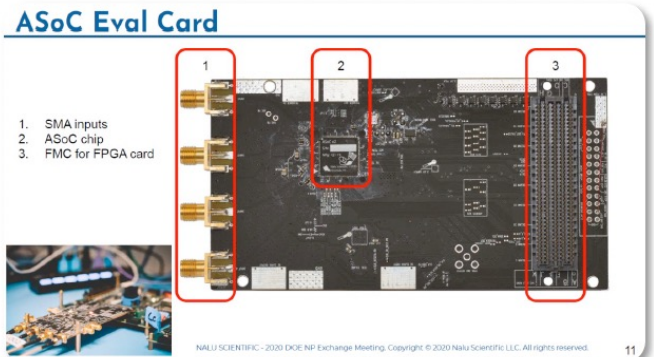

4 Channel and Analog Bandwidth 850 MHz

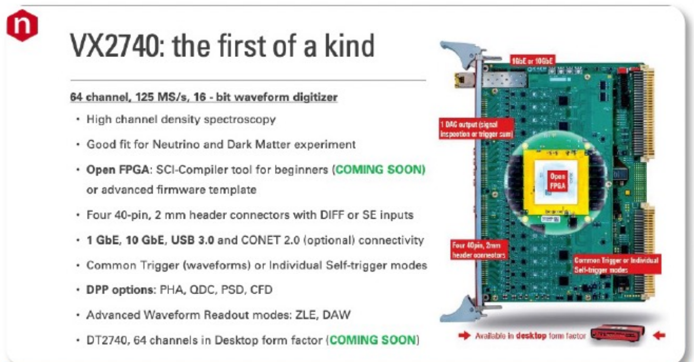

OPEN FPGA system

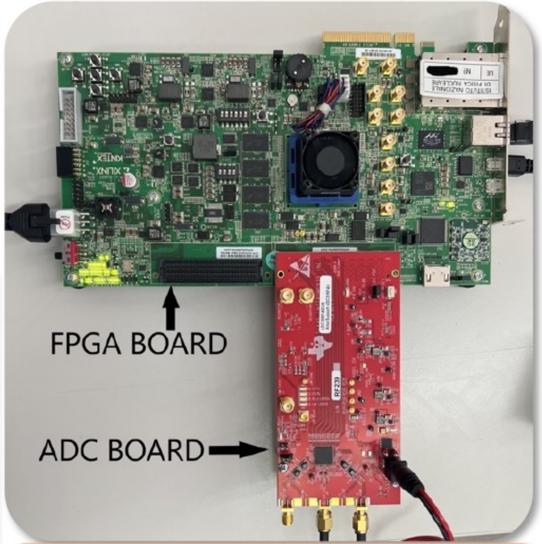

Xilinx Kintex UltraScale **FPGA** KCU105 Evaluation Kit **+ ADC dual channel** ADC32RF45EVM

- Understand how to best implement the data transfer to the DAQ, using **optical fiber with SFP + connectors** or **SFP + to RJ45 adapters** to use the new **10Gbit/s standard** (especially for (1) and (2)).

- Investigate the best way **to save information before the transfer** (we need it if a bottleneck during the transfer happens).

Summary/Conclusions

Good progress reported on:

- mechanical structure project
- testbeam data analysis
- data reduction and pre-processing
- simulation (geometry, performance, cluster counting)

Plenty of areas for collaboration:

- detector design, construction, beam test, performance
- local and global reconstruction, full simulation
- physics performance and impact
- etc.

Manpower, funding under continuous discussion

Thanks to all the contributors (many!)

Backup

2021/2022 testbeam: clusterization

CLUSTERIZATION algorithm: Reconstruction of Primary Ionization Clusters

- Merging of electron peaks in consecutive bins in a single electron to reduce fake electrons counting

- Contiguous electrons peaks which are compatible with the electrons' diffusion time (it has a $\sim\sqrt{t_{ElectronPeak}}$ dependence, different for each gas mixture) must be considered belonging to the same ionization cluster.

- Position and amplitude of the clusters corresponds to the position and height of the electron having the maximum amplitude in the cluster. → Poissonian distribution for the number of clusters!

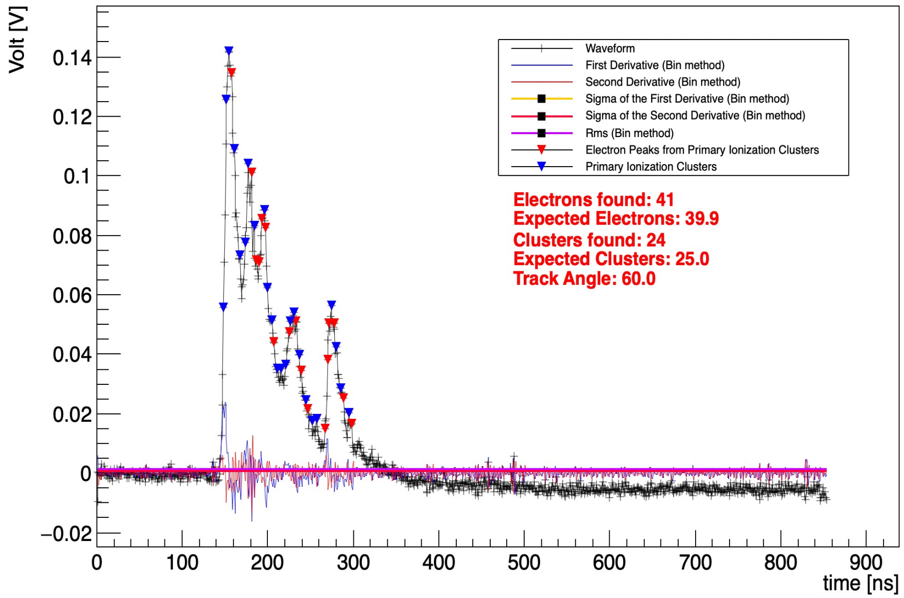

Electron per Clusters Distribution

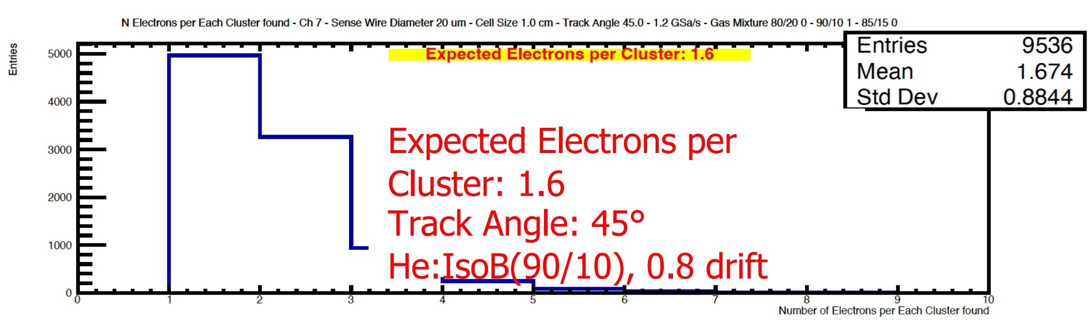

Sense Wire Diameter 20 um – Cell Size 1.0 cm – Track Angle 60° – 1.2 GSa/s – Gas Mixture He:IsoB 90/10 – 165 GeV

Track finding – local method for DCH only

Seeding from 3 hits in different layers with origin constraint

- Take any 2 free hits from different stereo layers with a gap (4 or 6 layers)
- Cross Point of 2 wires give Z-coordinate
- Select nearest free hits at middle (+-1) layer
- 2 hits from same stereo layer give initial angle in Rphi
- origin added with sigma Rϕ~ 1mm Z ~ 1mm
- Seeds constructed for all 2x2x2=8 combination of Left-Right pc

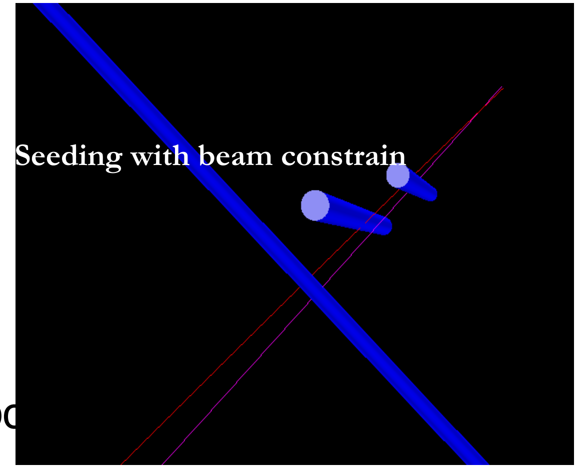

- Checked that at -4 (+-1) layer are available free hits with $\chi^2 < 16$
- Extrapolate and assign any compatible hits (by χ^2) from last to first hits
- Refit segment to reduce beam constraint
- Check quality of track segment:
  - χ^2/NDF < 4
  - number of hits found (>=7)
  - number of shared hits (<0.4Nfound)

Large combinatory:
local compatibility over different layers,
+ 1 from different stereo view

Mechanical structure: the FEM analysis

Studies made by using the Finite Element Method:

- Element to test: surface body modelled with Shell element, spokes with Beam element and cables with Truss element
- Load to apply: uniformly distributed line pressure
- Boundary conditions: fixing the surface of the outer cylinder (undeformable) or fixing the edge of the outer cylinder (deformable)
- Parametric study on mesh size

Design	Mesh	Total deformation Maximum		Equivalent Stress Maximum in Outer Cylinder			Equivalent Stress Average in Outer Cylinder			Maximum Axial Force	Equivalent Stress Maximum	Mesh Min	Mesh Average	Solution Elapsed	Number Mesh
No	Size	Model	OuterCylinder	Averaged	Unaveraged	Nodal diff	Averaged	Unaveraged	Nodal diff	Spokes	Cables	Quality	Quality	Time	Elements
DP 0	50	142.993	16.637	1763	3233	2932	223	286	201	12132	3197	0.13	0.80	5	189
DP 1	45	145.261	17.378	821	1824	1694	219	273	190	12139	2992	0.34	0.89	7	206
DP 2	40	139.848	15.347	1777	3293	2996	226	282	200	12126	3204	0.39	0.92	12	216
DP 3	35	139.495	15.478	1329	3262	2937	213	261	197	12145	3184	0.47	0.93	7	251
DP 4	30	138.848	15.258	1273	2367	2069	212	253	178	12219	2880	0.46	0.92	12	266
DP 5	25	142.349	16.348	1259	2249	1939	194	228	141	12175	2853	0.44	0.95	9	320
DP 6	20	139.726	15.968	2028	2994	2603	157	180	104	12233	3056	0.68	0.97	17	425
DP 7	15	130.568	14.311	1750	3104	3007	162	177	81	12559	3146	0.04	0.96	27	607
DP 8	10	135.217	15.275	2376	2497	2058	143	151	52	12368	3227	0.67	0.99	22	1120
DP 9	5	135.033	14.734	1976	2386	1908	140	144	34	12294	3246	0.60	0.99	77	3838
DP 10	4	133.568	15.002	1860	2249	2043	137	141	30	12476	3221	0.60	0.99	324	5900
DP 11	3	134.377	14.570	2042	2683	2330	139	141	26	12311	3225	0.67	0.99	291	10228
DP 12	2	137.256	15.212	1681	2156	1998	136	139	24	12243	3275	0.67	0.99	2149	22337
DP 13	1	133.266	13.931	2472	2570	1981	131	132	7	12283	3152	0.59	1.00	12892	85442

Mechanical structure: the FEM analysis

A full scale model is built with ANSYS Workbench and loaded with uniformly distributed line pressure.
Materials: carbon for spoke, stainless stell for cables

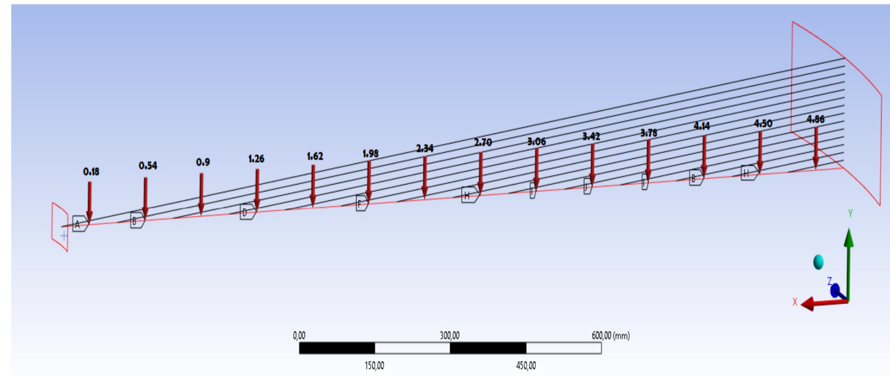

Linear analysis
HP: small deformations

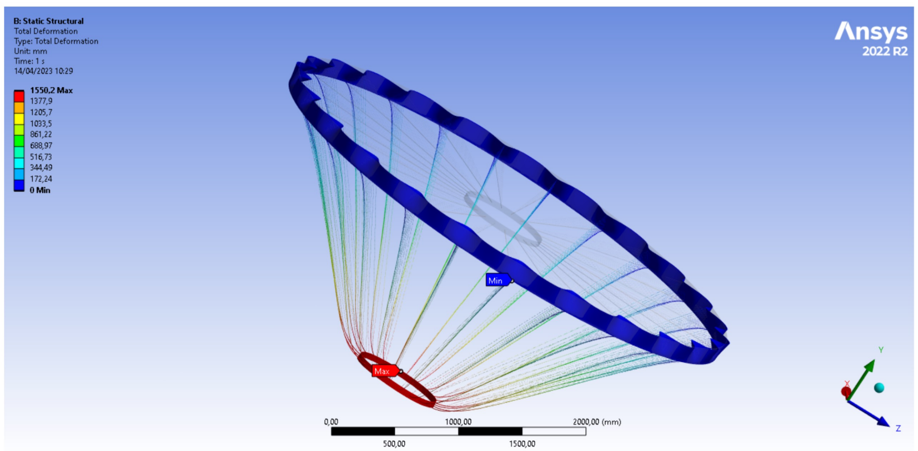

The maximum deformation occurs on inner cylinder 1550,2 mm (not realistic)

Non-Linear analysis
HP: Large strain, rotation, stress stiffening

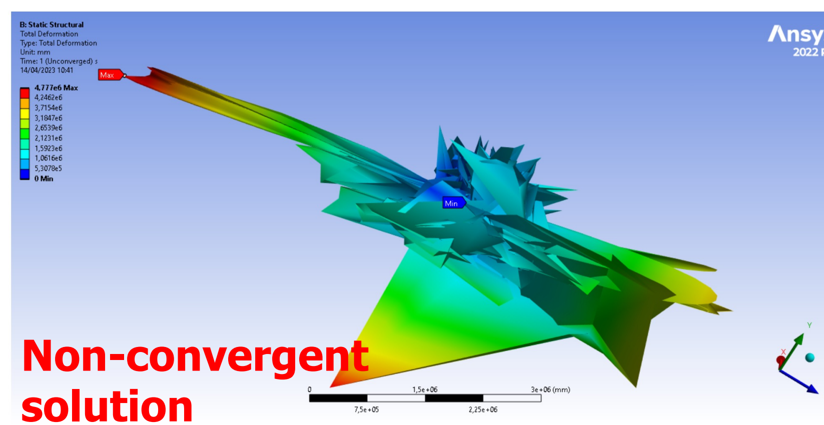

Non-convergent solution

Mechanical structure: the FEM analysis

Time stepping algorithm:

- the time step size are automatically determined in response to the current state of the analysis under consideration.
- estimate the next time step size Δt_{n+1}, based on current t_n and past analysis Δt_n conditions, and make proper load adjustments

The maximum deformation occurs on inner cylinder 133,27 mm (more realistic)

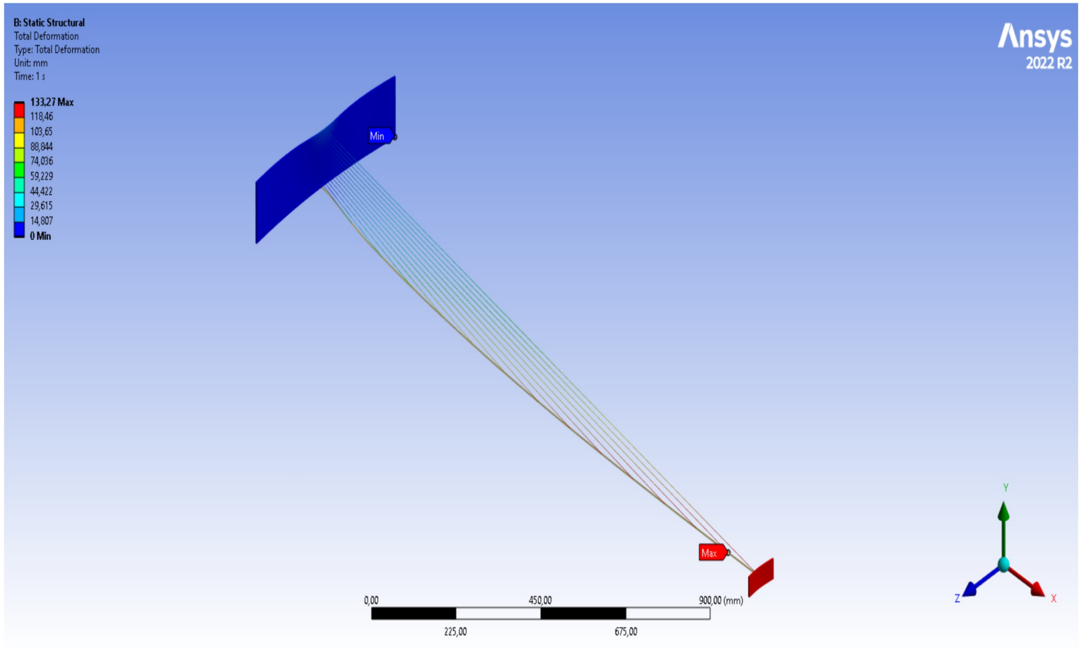

Mechanical structure: the FEM analysis

The model developed was validated with 3 different configurations:

1. Materials: composite for spokes and steel for cables
   Boundary conditions: fixing the lower edge of the outer cylinder.

2. Materials: composite for spokes and steel for cables
   Boundary conditions: fixing the surface of the outer cylinder.

3. Materials: Structural steel
   Boundary conditions: fixing the lower edge of the outer cylinder

	Edge fixed	Face fixed	Edge fixed
Material type	Composite and steel	Composite and steel	structural steel
Max. Total deformation in model (mm)	135.03	96.83	108.37
Max. Total deformation in outer cylinder (mm)	14.73	-	7.84
Min. Axial force in Spokes (N)	-365.87	-1957.80	-1312.40
Max. Axial force in Spokes (N)	12294.00	13497.00	13103.00
Max. Equivalent stress in Cables (MPa)	3245.70	3350.90	3330.50
Avg. Equivalent stress in Cables (MPa)	71.49	89.95	82.88
Max. Equivalent stress in Inner cylinder (MPa)	1646.70	1885.20	1952.90
Avg. Equivalent stress in Inner cylinder (MPa)	280.11	317.02	335.90
Max. Equivalent stress in Outer cylinder (MPa)	1976.00	-	1618.30
Avg. Equivalent stress in Outer cylinder (MPa)	139.77	-	224.33
Mass (kg) per sector	0.69587	0.69587	2.7773
Volume (mm³) per sector	3.54E+05	3.54E+05	3.54E+05

Best configuration

Cluster counting on a KCU105 + ADC ADC32RF45

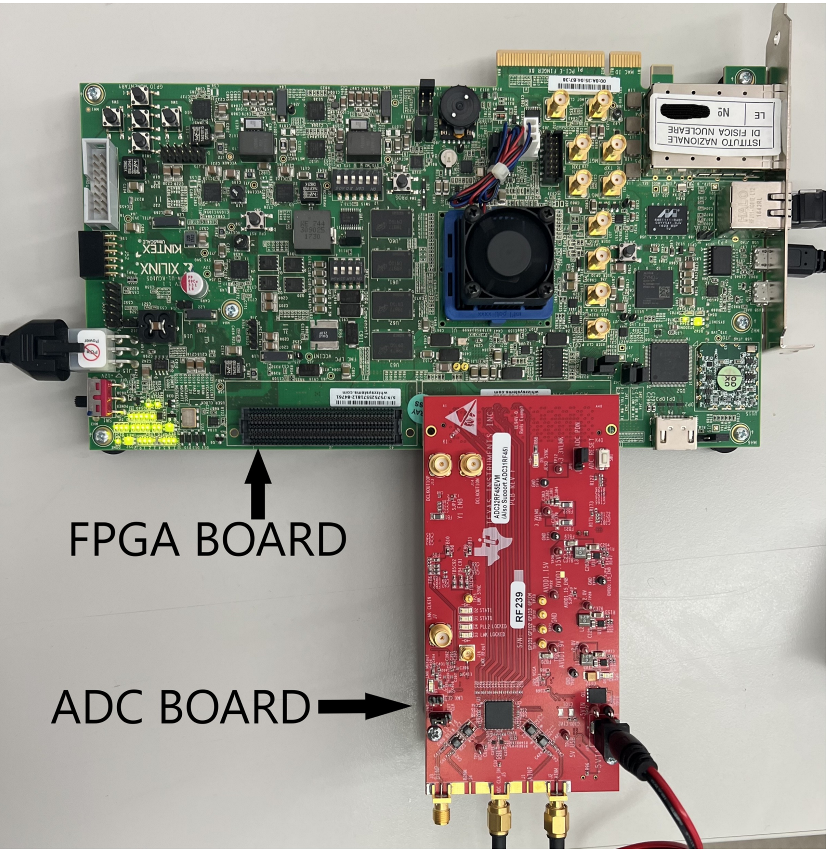

- We have transferred the old code of the single channel ADC made in the old framework to the xilinx new frameworks
- The communciation with the new ADC was carried out and some simulations on timming and power consumption (next slide)
- We are developing the code to use SFP + connections for the 10Gb standard
- The integration between the CCT algortymus block have to be terminated

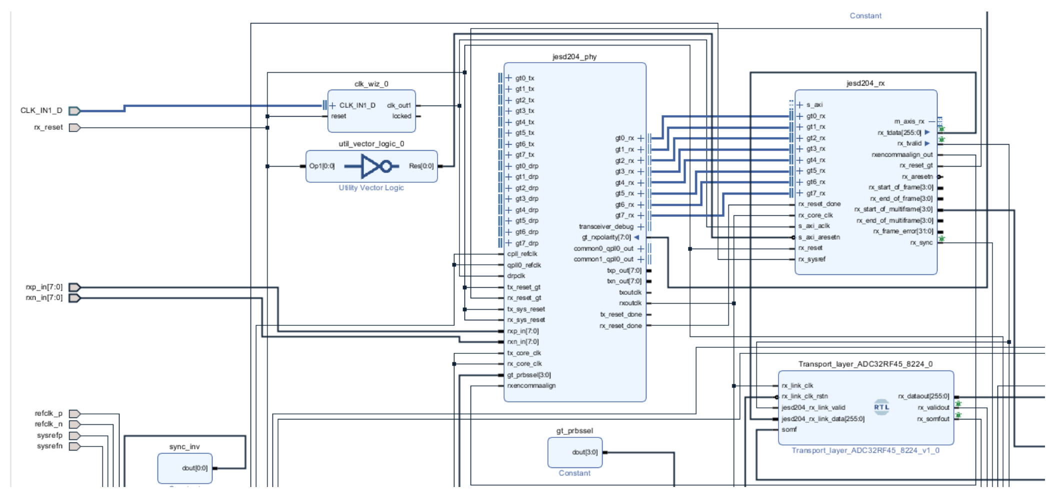

Cluster counting on a Naluscientifc ASoCV3

- At the end of June we received the board with the ASoCv3, We are currently testing it with a pulse generator
- The next step is to connect it to the LMH6522 amplifier (4 channel amplifier) to do some tests with some tubes
- Currently we cannot implement the algorithm directly because we do not have some IP of the source code, we are in contact with Naluscientific. We use their software to collect the signal (Naluscope)

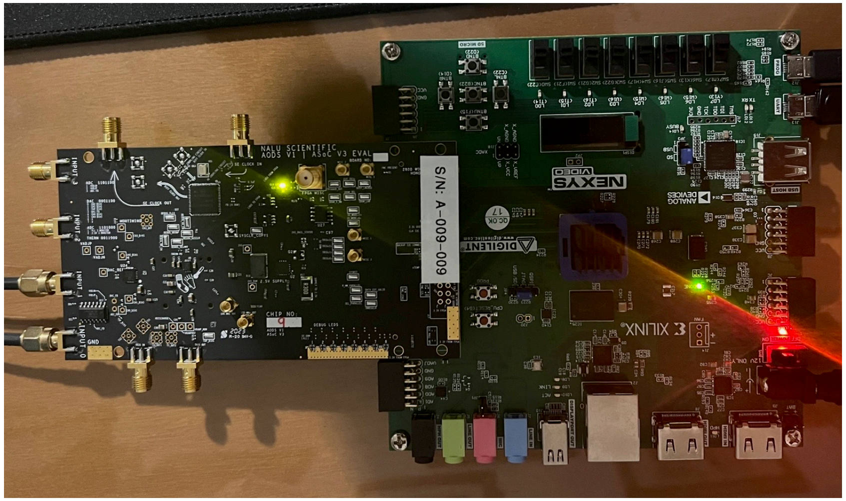

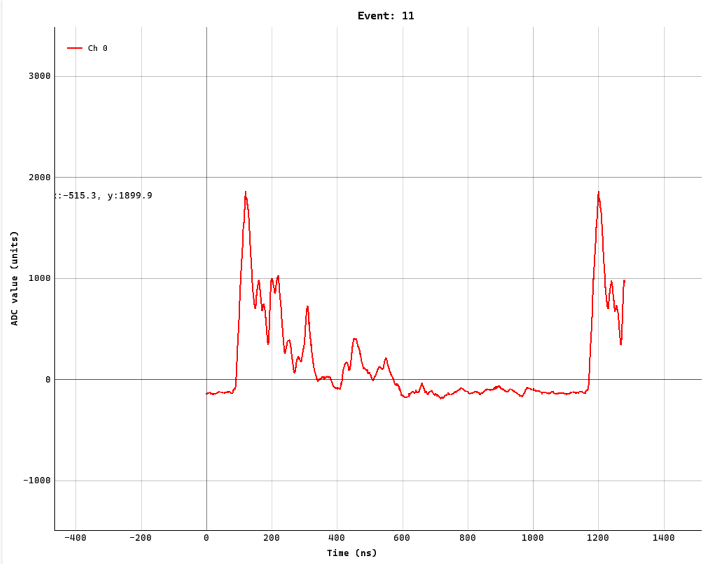

Cluster counting on a Caen VX2740

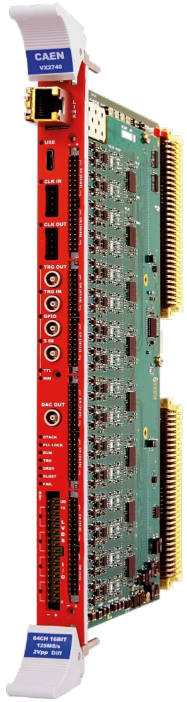

- At the end of June we also received the CAEN digitizer (not in the version we need because it is still under development)
- We are becoming familiar with the openFPGA SCICompiler software (released a few days ago) and we have a trial license with a timebomb that does not allow us to do excessive development.
- We are waiting for Caen to have a full license

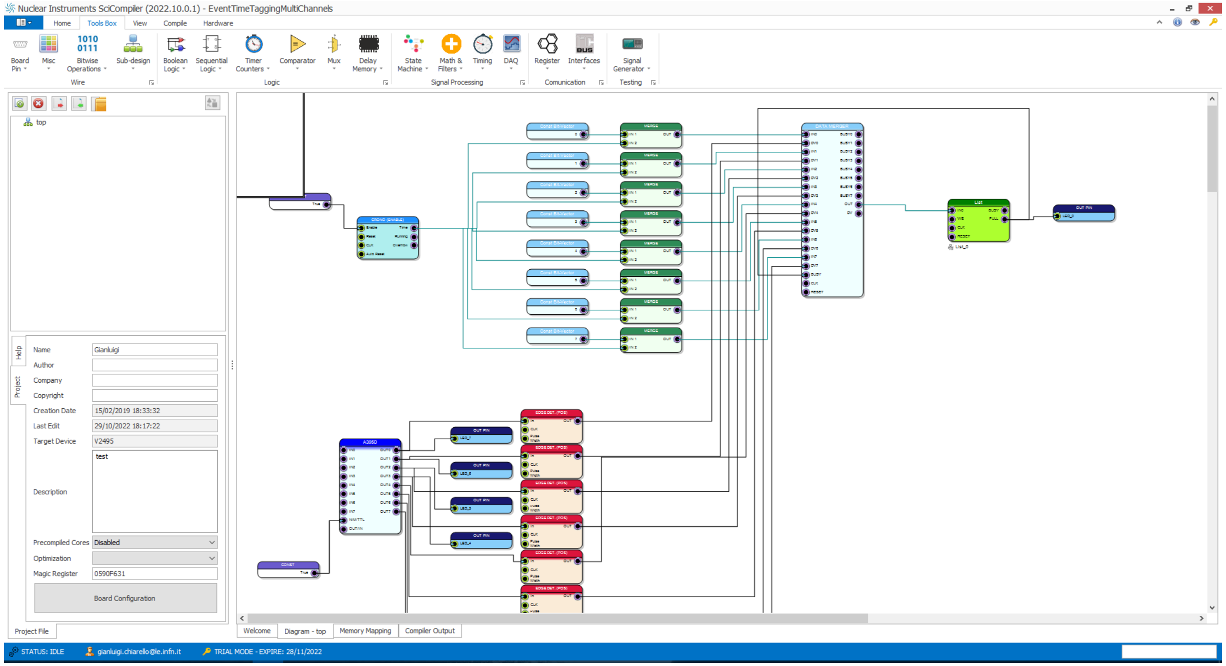

Board for cluster counting: new idea ML algorithm

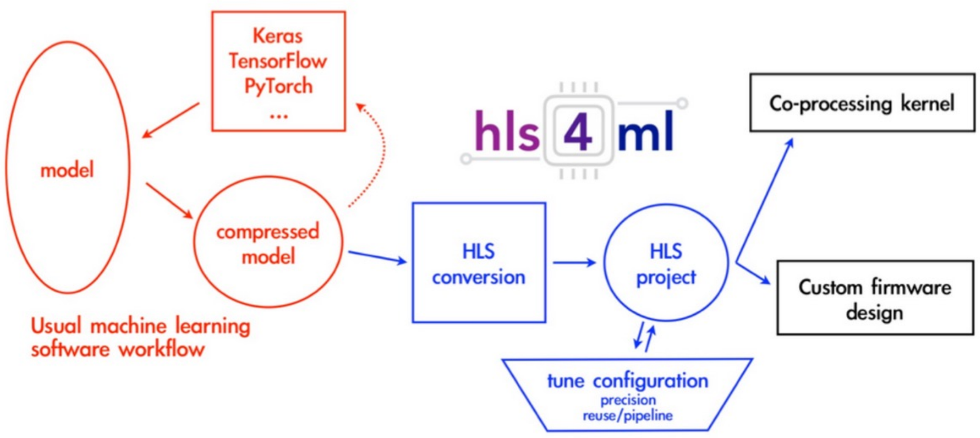

The first step required for the implementation of the neural network on the FPGA is the conversion of the high-level code used for the creation of the network (QKeras) into an High-Level Synthesis (HLS)

To accomplish this task, the hls4ml package will used.

A schematic workflow of hls4ml is illustrated in the figures.

1. The parts red indicates the usual software steps required to design a neural network for a specific task.
2. The blue section of the workflow is the task done by hls4ml, which translates the model into an HLS project that can be synthesised and implemented to run on an FPGA.

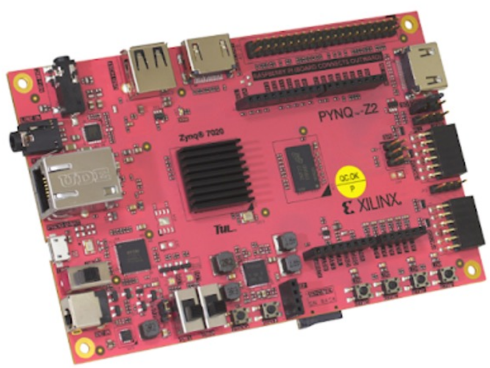

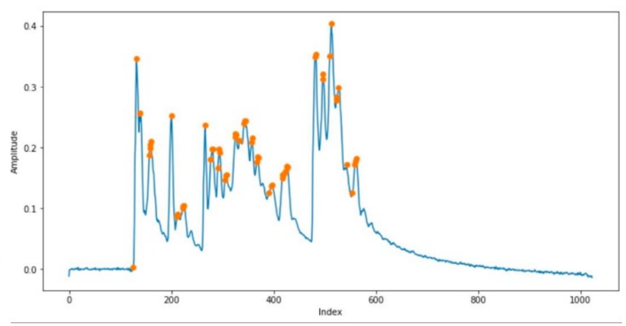

12

Detector simulation for IDEA

Geant4 and DD4HEP simulations of the IDEA geometry are available

- The DCH is simulated at a good level of geometry details, including detailed description of the endcaps; hit and digi creation (while track reconstruction code available in Geant4)

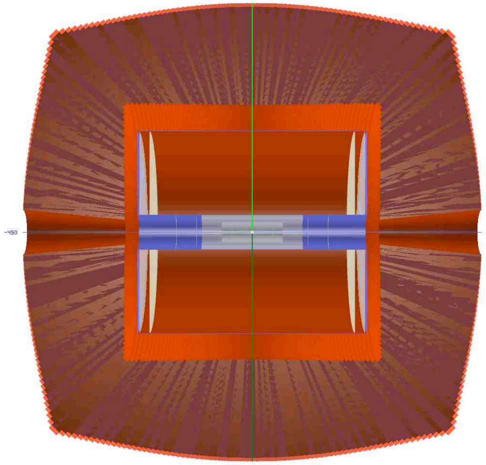

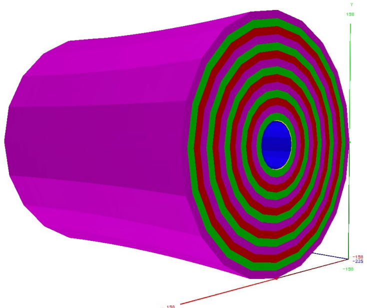

- SVX and Si wrapper are simulated too

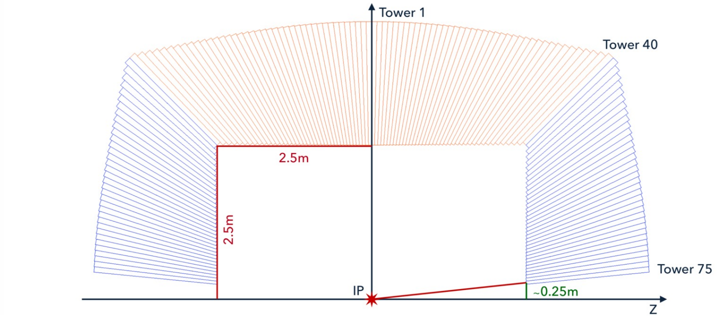

- solenoid is also simulated in a simple way

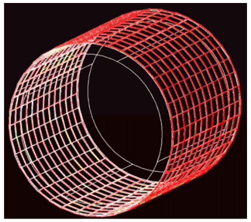

- Dual readout calorimenter simulated combining DR fibers and crystals (in a fully compensating segmented calorimeter)
- Muon detector: simulated with a cylindrical geometry

Track finding: performance of the current IDEA

For the Geant4 based simulation framework code:

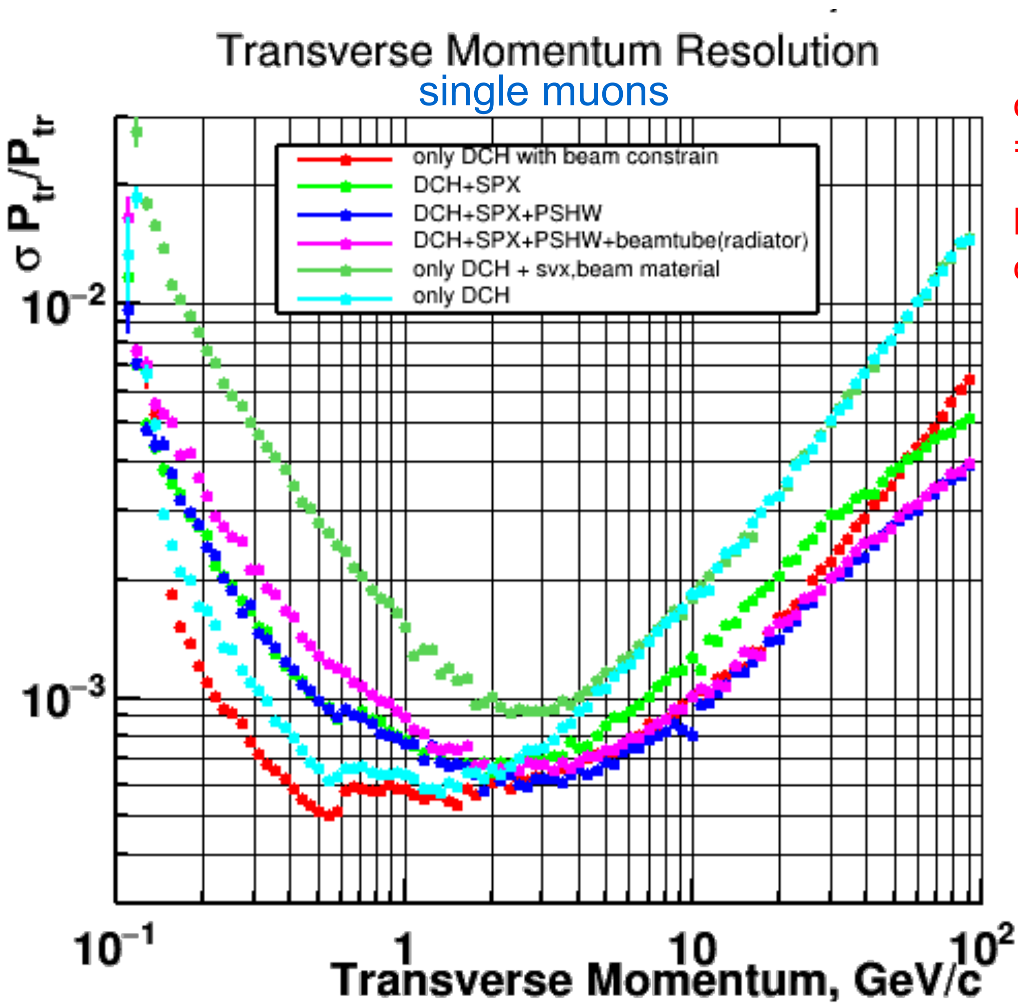

$\sigma(p_t)/p_t$ (100 GeV) $= 3\text{x}10^{-3}$

but new studies ongoing

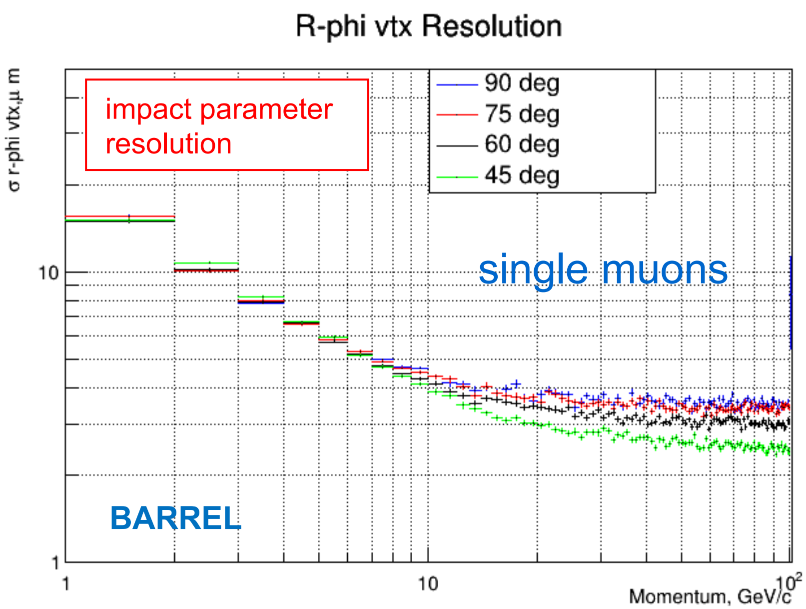

$\sigma(d_0)$ (100 GeV) = 2□m

Performance of the tracking with DCH